Journal of Pharmaceutical and Biomedical Analysis 93 (2014) 86–94

Contents lists available at ScienceDirect

Journal of Pharmaceutical and Biomedical Analysis

journal homepage: www.elsevier.com/locate/jpba

^{1}H nuclear magnetic resonance based-metabolomic characterization of Peucedani Radix and simultaneous determination of praeruptorin A and praeruptorin B

Yue-Lin Song [a], Wang-Hui Jing [a], Yan-Gan Chen [a], Yun-Fei Yuan [b], Ru Yan [a], Yi-Tao Wang [a,*]

[a] State Key Laboratory of Quality Research in Chinese Medicine, Institute of Chinese Medical Sciences, University of Macau, Macao, China
[b] State Key Laboratory for Conservation and Utilization of Subtropical Agro-bioresources, South China Agricultural University, Guangzhou, China

ARTICLE INFO

Article history:
Received 26 April 2013
Received in revised form 18 August 2013
Accepted 20 August 2013
Available online 31 August 2013

Keywords:
Peucedani Radix
Metabolomic profile
Quantitative ^{1}H NMR
Praeruptorin A
Praeruptorin B

ABSTRACT

As a widely used traditional herbal medicine, it is crucial to characterize the holistic metabolic profile of Peucedani Radix (Chinese name: Qian-hu). However, it is quite arduous to obtain the whole picture of chemical constituents appropriately with the existing analytical techniques that were based on HPLC–UV or LC–MS/MS system. In present investigation, nuclear magnetic resonance (NMR) spectroscopy coupled with principal components analysis (PCA) was introduced to metabolomic characterization of Qian-hu crude extracts without any chromatographic separation. In addition, the contents of praeruptorin A (PA) and proaeruptorin B (PB) in Qian-hu were simultaneously determined using quantitative ^{1}H NMR (q^{1}H NMR) spectroscopy. Eighteen reference compounds (**1**–**18**), which were purified from this herbal drug extract previously, were recruited for the assignment of the protonic signals in the ^{1}H NMR spectra. Following PCA, 15 batches of Peucedani Radix were divided into two groups (I and II), and angular-type pyranocoumarins, in particular PA and PB, as well as 5-methoxycoumarin were demonstrated as the predominant markers being responsible for the distinguishment of Qian-hu from different districts. The contents of the two analytes (PA & PB) were calculated by the relative ratio of the integral values of the target peak for each compound to the known amount of the internal standard, formononetin (IS). The lower limits of quantitation were determined as 19.5 μg/mL for both PA and PB. The quantitative results indicated that the contents of PA and PB showed quite variable qualities among different extract samples. Above all, ^{1}H NMR spectroscopy, that could not only provide comprehensive profiles of the metabolites but also achieve convenient determination of praeruptorin A and praeruptorin B, is a promising means for evaluating the medicinal samples of Peucedani Radix.

1. Introduction

Peucedani Radix (Qian-hu in Chinese), the dried roots of *Peucedanum praeruptorum* Dunn (Apiaceae) [1], has been widely employed for the treatment of cough with thick sputum and dyspnoea, nonproductive cough and upper respiratory infections [2] for centuries in China. On modern pharmacological models, this herbal drug was highly marked for tracheal and pulmonary arteries relaxant [3], coronary dilatory [2], myocardial protective [4], antitumor-promoting [5] and anti-inflammatory [6] activities, *etc.*

There are several classes of compounds reported in Peucedani Radix, and the major constituents are angular-type pyranocoumarins (APs) that are widely believed to make the main contribution to the pharmacological properties of Qian-hu [7]. This kind of components always comprises a khellactone skeleton with varied acyl substituents at C-3′ and/or C-4′ positions. Many APs were drawing increasing interest due to their strong hypotensive activity typically through acting as a calcium channel blocker and/or a potassium channel opener [3,8]. Recent studies also revealed the prospect of these pyranocoumarins in chemotherapy based on their pharmacological properties of antiproliferation, cytotoxicity and apoptosis-induction [9,10] as well as P-glycoprotein (P-gp) expression suppressing effects [11,12].

As the quality indicators of Qian-hu and related herbal products documented in Chinese Pharmacopoeia (2010 version) [1], praeruptorin A (PA) and praeruptorin B (PB) have been reported diverse biological activities by a great amount of evaluations. PA was intensively proved to be a novel calcium channels blocker [4] and a potassium channel opener [8], and showed the prospects in prevention and therapy of cardiac diseases. It also exhibited antiplatelet aggregative [13], anti-proliferative [13] and anti-inflammatory effects [14,15]. Moreover, the neuroprotective effect of PA was also reported recently [16]. On the other side, PB, as an analogue of PA, has also drawn extensive attention in recent

* Corresponding author. Tel.: +853 8397 4691; fax: +853 2884 1358.
E-mail address: ytwang@umac.mo (Y.-T. Wang).

0731-7085/$ – see front matter © 2013 Published by Elsevier B.V.
http://dx.doi.org/10.1016/j.jpba.2013.08.021

years since it was found to possess some other specific pharmacological effects such as inhibition of tumour promoter induced phenomenon *in vitro* [17] and potent anti-inflammatory action in addition to the above-mentioned similar activities of PA [18].

Over the recent years, with the development of much higher magnetic fields with higher sensitivity, one- and two-dimensional NMR spectroscopy has been adopted as routine implements for the analyses of complex matrices [19]. Especially, ^{1}H NMR spectroscopy was proved as a robust and high-throughput analytical method that can provide not only a significant amount of structural information but also a comprehensive profile of the sample in terms of its chemical constituents in just a single measurement [20]. And more fortunately, the availability of various mathematical tools and softwares also provides conveniences for multivariate data analysis, such as principle component analysis (PCA) and partial least squares discriminant analysis (PLS-DA). In previous reports, NMR spectroscopy has been employed for chemotaxonomic evaluation of this traditional Chinese herbal drug [21–24], and the results revealed that ^{1}H NMR spectroscopy is a quick, simple and reliable approach to distinct Qian-hu with other similar herbal drugs, including the species of *P. decursivi, P. medicun, P. rublicanle* and so on, while angular-type pyranocoumarins, in particular PA, were adopted as the chemical markers for recognition. However, neither the assignment of the protonic signals in the ^{1}H NMR spectra nor quantitative analysis of chemical components in Peucedani Radix has been achieved using NMR spectroscopy.

In general, traditional quantitative techniques, HPLC–UV and LC–MS/MS for instance, make use of chromatographic separation of components in the crude extract and determination of the separated components with the adoption of specific detectors, indicating the demands of complicated sample preparation, large amounts of solvents and/or time-consuming procedures. On the contrary, quantitative ^{1}H NMR (q^{1}H NMR) is an ideal strategy to overcome the shortcomings which general quantification techniques usually encounter, thus being regarded as a promising tool for the quality control of herbal drugs. In the past decade, q^{1}H NMR has been widely introduced for the qualitative and/or quantitative analysis of active ingredients in complex plant extracts, such as, quantitative determination of artemisinin in *Artemisia annua* [25], sesquiterpene lactones in *Arnica Montana* [26], ephedrine analogues in *Ephedra species* [27], and hypericin and pseudohypericin in *Hypericum perforatu* [28].

In the case of Peucedani Radix, the quality standard was proposed by Zhang et al. adopting HPLC–UV [25] to monitor PA and PB, without concerning the other components. Thus, a great risk of counterfeit drug is thus, led by the absence of chemical profile.

Therefore, in current investigation, as an important part of our continuous work on Peucedani Radix, we aim to: (1) characterize the metabolic profile of Qian-hu using the detailed signal assignment information based on ^{1}H NMR spectra combining with multivariate statistical analysis; (2) simultaneous determination of praeruptorin A and praeruptorin B using quantitative ^{1}H NMR spectroscopy.

2. Experimental

2.1. Chemicals

Praeruptorin A (PA, **2**), praeruptorin B (PB, **3**) and (+)-praeruptorin E (PE, **4**) (purity >99% for all compounds) were purchased from Shanghai Traditional Chinese Medicine Research Centre (Shanghai, China). Other 10 angular-type pyranocoumarins, including *cis*-khellactone (**1**), *cis*-3′-acetyl-4′-angeloylkhellactone (**5**), *cis*-3′-isovaleryl-4′-acetylkhellactone (**6**), *cis*-3′-angeloyl-4′-senecioylkhellactone (**7**), *cis*-3′,4′-diisovalerylkhellactone (**8**), *trans*-3′-angeloylkhellactone (**9**), 3′-angeloyloxy-4′-oxo-3′,4′-dihydroseselin (**10**), *trans*-4′-angeloylkhellactone (**11**), *trans*-3′-acetyl-4′-isobutyrylkhellactone (**12**), *trans*-3′-acetyl-4′-angeloylkhellactone (**13**) were isolated from Peucedani Radix in our laboratory [29]. 5-Methoxycoumarin (**14**), 5,8-dimethoxycoumarin (**15**), 7-hydroxylcoumarin (**16**), stigmasterol (**17**) and palmitic acid (**18**) were also identified from this herbal medicine. All the chemical structures (Fig. 1) were determined on the basis of NMR spectra (Supplemental figures) and LC–MS/MS spectral data. Moreover, formononetin which was presented by Dr. Qingwen Zhang in our institute, served as internal standard (IS).

$CDCl_3$ (deuterium abundance, 99.96 atom% deuterium) containing 0.03% trimethylsilane (TMS) was purchased from Cambridge Isotope Laboratories Inc. (Miami, FL, USA). Analytical grade $CHCl_3$ was obtained commercially from Kaitong Chemical Co. Ltd. (Tianjin, China).

Table 1
The contents (mg/g) of praeruptorin A and praeruptorin B in Peucedani Radix from different districts (PR1–15).

	Habitats	PA (mg/g)[a]	RSD%[b]	PB (mg/g)[a]	RSD%[b]
PR1	Anguo, Anhui (wild)	23.07	4.7	20.73	3.7
PR2	Anguo, Anhui (cultivate)	16.61	3.9	13.42	5.3
PR3	Taiyuan Shanxi (1)	51.39	5.7	10.53	5.9
PR4	Taiyuan Shanxi (2)	12.15	4.3	7.458	5.5
PR5	Chongqing	12.69	4.1	2.590	5.3
PR6	Chengdu, Sichuan	3.769	5.5	2.172	3.6
PR7	Hangzhou, Zhejiang	5.922	6.0	N.D.	N.A.
PR8	Hongkong	5.327	3.7	2.150	4.5
PR9	Macao	0.01686	5.8	0.2627	5.3
PR10	Nanchang, Jiangxi	15.78	3.8	2.557	4.4
PR11	Wenzhou, Zhejiang (1)	44.90	5.8	5.609	4.8
PR12	Wenzhou, Zhejiang (2)	N.D.	N.A.	N.D.	N.A.
PR13	Guangzhou, Guangdong	37.26	5.6	2.847	4.6
PR14	Shanghai	55.21	4.9	19.51	3.6
PR15	Linfen Shanxi	N.D.	N.A.	N.D.	N.A.

N.D.: not detected. N.A.: not applied.
[a] The mean content of triplicate.
[b] RSD% of triplicate.

2.2. Plant materials

A total of 15 batches of Peucedani Radix (PR1–15) were collected from 15 different locations (Table 1) in China. The botanical origins of the material were authenticated by Professor Pengfei Tu from Department of Natural Medicines, Peking University Health Science Center, Beijing, China, and the voucher specimens were deposited at the Institute of Chinese Medical Sciences, University of Macau, Macao SAR, China. All the crude materials were dried using a universal oven with forced convection (FD115, Tuttlingen, Germany) at 40 °C for 4 days.

2.3. Preparation of samples for NMR spectroscopic analysis

The dried roots were crushed into powder with sample mill (model YF102, Ruian Yongli Pharmacy Machinery, China), following by passing through an 80 mesh sieve. And then, the pulverized crude materials (accurate quantity about 200 mg) were extracted with 5 mL of $CHCl_3$ using ultrasonication for 30 min at 40 °C. Each extracting solution was centrifuged at 10 000 × *g* for 10 min, and the supernatant was filtered through a 0.45 μm nylon membrane filter (Tianjin Jinteng Experiment Equipment Co., Ltd, China). An aliquot (2.5 mL) of the filtrate was transferred into another tube and evaporated under nitrogen flow at 25 °C. Following evaporation, the residues were reconstituted with 600 μL of $CDCl_3$, and quickly transferred into 5-mm tubes (Norell ST500-7) for NMR analysis.

All the reference compounds were also dissolved using 600 μL of $CDCl_3$ in 5-mm tubes (Norell ST500-7) and analyzed parallelly

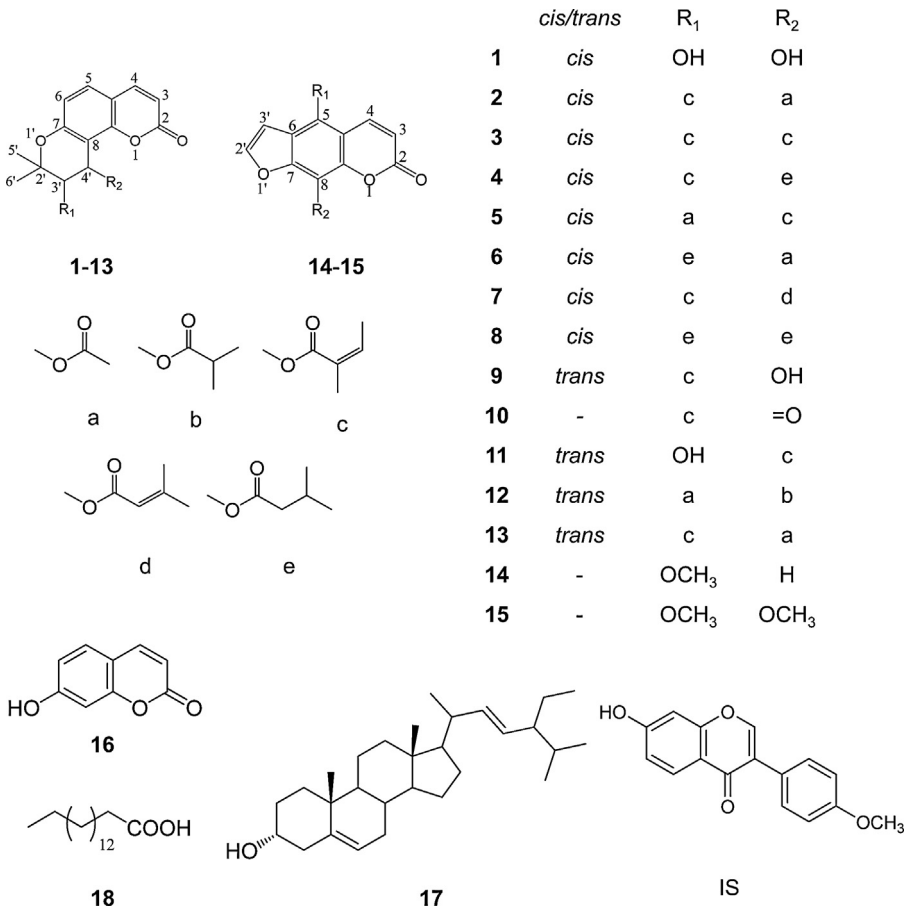

	cis/trans	R_1	R_2
1	*cis*	OH	OH
2	*cis*	c	a
3	*cis*	c	c
4	*cis*	c	e
5	*cis*	a	c
6	*cis*	e	a
7	*cis*	c	d
8	*cis*	e	e
9	*trans*	c	OH
10	-	c	=O
11	*trans*	OH	c
12	*trans*	a	b
13	*trans*	c	a
14	-	OCH_3	H
15	-	OCH_3	OCH_3

Fig. 1. Chemical structures of compounds **1**–**18** and internal standards (IS). *cis*-khellactone (**1**), praeruptorin A (**2**), praeruptorin B (**3**), praeruptorin E (**4**), *cis*-3′-acetyl-4′-angeloylkhellactone (**5**), *cis*-3′-isovaleryl-4′-acetylkhellactone (**6**), *cis*-3′-angeloyl-4′-senecioylkhellactone (**7**), *cis*-3′,4′-diisovalerylkhellactone (**8**), *trans*-3′-angeloylkhellactone (**9**), 3′-angeloyloxy-4′-oxo-3′,4′-dihydroseselin (**10**), *trans*-4′-angeloylkhellactone (**11**), *trans*-3′-acetyl-4′-isobutyrylkhellactone (**12**), *trans*-3′-acetyl-4′-angeloylkhellactone (**13**), 5-methoxycoumarin (**14**), 5,8-dimethoxycoumarin (**15**), 7-hydroxycoumarin (**16**), stigmasterol (**17**), palmitic acid (**18**) and formononetin (IS).

with extract samples to assist the assignment of the signals in ^{1}H NMR spectra of extracts.

2.4. 1D and 2D NMR experiments

To acquire comparable spectra, all the extract and reference samples were analyzed using the identical set of acquisition parameters. 1D and 2D NMR spectra were recorded at 298.2 K on a Bruker 600 MHz AVANCE IINMR spectrometer at 600.13 MHz proton frequency (Bruker, Karlsruhe, Germany) equipped with a TCI cryoprobe and a *Z*-gradient system. $CDCl_3$ was used for internal lock purpose, while TMS was adopted for the internal reference of δ 0.00. For 1D-^{1}H NMR spectra a total of 32 768 data points were recorded covering a spectral window of 9 615 Hz. 128 scans of a standard one-pulse sequence with 30° flip angle for excitation was adopted. Data was zero-filled to 65 536 points and an exponential window function with a line broadening factor of 0.3 Hz was applied prior to Fourier transformation. The chemical shifts of all the spectra were normalized with the signal from TMS at δ 0.00. To confirm the assignments, two-dimensional (2D) NMR spectra, such as ^{1}H–^{1}H correlation spectroscopy (^{1}H–^{1}H COSY), nuclear Overhauser enhancement spectroscopy (NOESY), total correlation spectroscopy (TOCSY), ^{1}H–^{1}H *J*-coupling resolved spectroscopy (^{1}H–^{1}H *J*-resolved), heteronuclear single quantum coherence spectroscopy (HSQC), and heteronuclear multiple bond correlation spectroscopy (HMBC) were also recorded on chosen samples using default Bruker programmes.

Initialized data processing was carried out with BRUKER TOPSPIN 2.1 software. An exponential function with LB = 0.3 Hz was applied. The Free Induction Decay (FID) signals were Fourier transformed (FT) and all the spectra were automatically phased and baseline corrected. The resulting spectra were aligned to right or left shifting as necessary using TMS signal as the reference. Data analysis was achieved with MestReNova 5.3.1 software package (Mestrelab Research SL).

2.5. Multivariate statistical analysis of NMR spectra

^{1}H NMR spectra were bucketed with equal bin width of 0.04 ppm over the range of δ 0.5–8.5 ppm after phase and baseline corrections. The spectral regions at δ 1.25–1.35 and δ 7.23–7.31 were excluded from the analyses to eliminate the effects of water suppressions and residual $CDCl_3$ followed by normalization to the total spectral area, respectively. And then, the data sets were imported and subjected to multivariate statistical analysis using SIMCA-P$^+$ software (version 13.0, Umetrics). Unit variance (UV) scaling methods and principal components analysis (PCA) was performed for the data sets, subsequently.

2.6. Quantitative ^{1}H NMR spectroscopy of praeruptorin A and praeruptorin B in Peucedani Radix

The longitudinal relaxation time (T_1) values of the diagnostic working protonic signals were optimized as 2.13 s and 2.07 s

for PA and PB, respectively. Therefore, relaxation time (d_1) was set as 10 s due to the higher T_1 offered by praeruptorin A, corresponding that d_1 was generally recommended five folds more than T_1. 64 scans were performed for each sample, while the other parameters were set as default in standard procedure. Accurately weighed PA and PB were mixed in 600 μL of $CDCl_3$ that contained 0.150 mg/mL of IS, to afford corresponding stock standard solutions (5 mg/mL). PR1–PR15 (200.00 mg for each batch) were treated using the method mentioned above and the residues were also dissolved using 600 μL of $CDCl_3$ containing 0.150 mg/mL of IS to prepared quantitative extract samples, respectively. The protons (4′-H) of PA and PB were chosen for quantitative analysis since the corresponding signals gave intense doublet peaks (J = 5.0 Hz) in a lower magnetic field and not overlap with other signals, while the singlet signal (2-H) exhibited at 7.93 ppm of IS (formononetin) was adopted as internal standard signal. A series of standard working solutions were obtained by consecutively dilution of the stock solutions using $CDCl_3$ to obtain the regressive calibration curves, limits of detection (LODs) and limits of quantitation (LOQs). Nine concentration levels of the solution were analyzed in triplicate, and then the calibration curves were constructed by plotting the ratios of the peak areas of each standard to IS *versus* the concentration level of each analyte. LOD was evaluated at a signal-to-noise (S/N) ratio of 3, while LOQ was evaluated at an S/N value of 10. Recovery samples were carried out by spiking high, medium and low concentration levels of standard mixture solutions to 100.00 mg of PR1, being extracted by 2.5 mL $CHCl_3$ and being dissolved using 600 μL of $CDCl_3$ containing 0.150 mg/mL of IS. Each level of recovery sample was prepared in triplicate. The average recoveries were counted by the formula: recovery (%) = (amount found − original amount)/amount spiked × 100%.

Precision, repeatability and stability assays were performed to validate the established method thoroughly, and the relative standard deviation (RSD) had been used to assess the results. PR1 was chosen and detected for six times continuously to carry out precision and repeatability assays. Stability study was achieved by detecting the same sample at different time points within 24 h.

The contents of the two analytes in Qian-hu samples were calculated using the following equation: [30]

$$\text{content(mg/g)} = \frac{A_x}{A_{IS}} \times \frac{N_{IS}}{N_x} \times \frac{M_x}{M_{IS}} \times \frac{W_{IS}}{W_x} P_{IS}$$

where A_x and A_{IS} represent the integral areas of the analyte and internal standard (IS), respectively; N_{IS} and N_x correspond to the numbers of spinning protons of internal standard and the analyte, respectively; M_x and M_{IS} are the molecular masses of the analyte and IS, respectively; W_{IS} is the weighed mass of IS, while W_x is the weighed mass of the analyte; P_{IS} is the purity of the standard (P_{IS} = 95%).

3. Results and discussion

3.1. Identification of chemical components in Peucedani Radix

Among the available analytical techniques generally used in metabolomics, NMR and MS-based methods are usually acknowledged to be the reasonable choices. NMR spectroscopy, in particular ^{1}H NMR, possesses superiorities unsurpassed by other techniques, such as the ease of simultaneous detection of diverse groups of metabolites in a relatively short measuring time, non-selectivity and convenient sample preparation. Herein, ^{1}H NMR was adopted for metabolomic study of Qian-hu and the assignment of signals in ^{1}H NMR spectra was performed on the basis of the reference compounds recognized from the extract. In spite of the relative ease of NMR method implementation and the available of reference compounds, signal overlapping does constitute an obstacle for identifying each metabolite in the complex matrices. This problem was partly solved in current study by acquiring various 2D spectra including ^{1}H–^{1}H J-resolved, COSY, TOCSY, NOESY, HSQC and HMBC (data not shown).

The identification of chemical constituents in Peucedani Radix was achieved by analysis of ^{1}H NMR spectra carefully. Previous literatures revealed that the main active ingredients of this herbal medicine were angular-type pyranocoumarins. Therefore, the chemical identification mainly concerned on this type of components in present investigation. Due to the similar structures of these PAs (Fig. 1), the protonic signal overlapped each other in ^{1}H NMR spectra. Therefore, most of the metabolites were tentatively identified and assigned by the means of comparing with the spectroscopic data of the components (Supplemental figures, Figs: S1–S18) obtained from this medicinal herb in our group previously (Fig. 1). The protonic signals of the identified components were assigned by analyzing each pure compound separately, and the assignment of the protonic signals was elucidated in Table 2. In addition, various two dimensional spectra were used to supply supporting information for our identification.

As the major type of constituents, the signals that were assigned to the khellactone-skeleton of those angular-type pyranocoumarins were observed obviously, including: δ 6.20–6.30 (3-H), 7.55–7.65 (4-H), 7.30–7.40 (5-H), 6.75–6.85 (6-H), 5.30–5.40 (3′-H), 6.55–6.75 (4′-H), 1.40–1.50 (5′, 6′-CH_3) (Fig. 2). Further, 3″-H of the angeloyl moiety at C-3′ position was normally observed around δ 6.12, while 3‴-H of the angeloyl moiety at C-4′ position was always exhibited around δ 6.03 (Fig. 2). The methyl groups that were linked to olefinic carbons of the acyl groups, 4″,5″,2‴-CH_3 of PA for instance, were normally observed between δ 1.80 and δ 2.15.

Most of the identified APs belonged to *cis*-khellactone derivates, PA (**2**), PB (**3**) and PE (**4**) for instance. The coupling constant between H-3′ and H-4′ of these components was observed at about 5.0 Hz due to the *cis*-configuration of C-3′ and C-4′. The difference of these APs occurred at the acyl substituents at C-3′ and C-4′ positions and the chemical shifts of the protons linked to C-3′ and C-4′ thus exhibited variations on account of the impact from those acyl substituents (Fig. 2). PA (**1**) was mentioned as the major component in *P. praeruptorum* [31], and the signals including: δ 6.25 (3-H, 1H, d, J = 9.5 Hz), 7.61 (4-H, 1H, d, J = 9.5 Hz), 7.35 (5-H, 1H, d, J = 8.6 Hz), 6.81 (6-H, 1H, d, J = 8.6 Hz), 5.42 (3′-H, 1H, d, J = 5.0 Hz), 6.61 (4′-H, 1H, d, J = 5.0 Hz), 1.45 (5′-H, 3H, s), 1.49 (6′-H, 3H, s), 6.14 (3″-H, 1H, q, J = 7.2 Hz), 1.97 (3H, d, J = 7.2 Hz), 1.88 (3H, s) and 2.12 (2‴-H, 3H, s) could be found in the ^{1}H NMR spectrum (Table 2 and Fig. 2). Similarly, the signals of PB and PE, which was also reported as the main constituents [31,32], were obviously detected in the spectrum (Table 2), including δ: 6.23 (3-H, 1H, d, J = 9.5 Hz), 7.60 (4-H, 1H, d, J = 9.5 Hz), 7.37 (5-H, 1H, d, J = 8.6 Hz), 6.82 (6-H, 1H, d, J = 8.6 Hz), 5.46 (3′-H, 1H, d, J = 5.0 Hz), 6.72 (4′-H, 1H, d, J = 5.0 Hz), 1.47 (5′-H, 3H, s), 1.51 (6′-H, 3H, s), 6.13 (3″-H, 1H, q, J = 7.2 Hz), 2.00 (4″-H, 3H, d, J = 7.2 Hz), 1.87 (5″-H, 3H, s), 6.03 (3‴-H, 1H, q, J = 7.2 Hz), 1.98 (4‴-H, 3H, d, J = 7.2 Hz), 1.85 (5‴-H, 3H, s) for PB, and δ 6.25 (3-H, 1H, d, J = 9.6 Hz), 7.60 (4-H, 1H, d, J = 9.6 Hz), 7.35 (5-H, 1H, d, J = 8.6 Hz), 6.81 (6-H, 1H, d, J = 8.6 Hz), 5.41 (3′-H, 1H, d, J = 4.8 Hz), 6.63 (4′-H, 1H, d, J = 4.8 Hz), 1.45 (5′-H, 3H, s), 1.48 (6′-H, 3H, s), 6.13 (3″-H, 1H, q, J = 7.2 Hz), 1.98 (4″-H, 3H, d, J = 7.2 Hz), 1.89 (5″-H, 3H, s), 2.20, 2.28 (2‴-H, each 1H, m), 2.14 (3‴-H, 1H, m), 0.97 (4‴-H, 5‴-H, 6H, d, J = 7.2 Hz) for PE, under the help of various 2D-NMR spectra. Interestingly, the chemical shifts of H-4′exhibited big variations among these three analogues, suggesting a bright prospect for the performance of quantitative ^{1}H NMR spectrometry. Owing to the possession of higher areas of the respectively characteristic signals, PA and PB were definitely regarded as the major constituents. The peak at δ 5.23 (4′-H, 1H, d, J = 5.0 Hz) was detected as the characteristic protonic signals of *cis*-khellactone (**1**) (Fig. 2), which was the skeleton

Table 2
Metabolites identified from ^{1}H NMR and 2D NMR spectra ($CDCl_3$ + 0.03% TMS) of Peucedani Radix and the assignment of protonic signals.

Metabolite	Assignment of protonic signals
1	6.27 (3-H, 1H, d, *J* = 9.5 Hz), 7.67 (4-H, 1H, d, *J* = 9.5 Hz), 7.34 (5-H, 1H, d, *J* = 8.6 Hz), 6.81 (6-H, 1H, d, *J* = 8.6 Hz), 3.89 (3′-H, 1H, d, *J* = 5.0 Hz), 5.23 (4′-H, 1H, d, *J* = 5.0 Hz), 1.42 (5′-H, 3H, s), 1.48 (6′-H, 3H, s)
2	6.25 (3-H, 1H, d, *J* = 9.5 Hz), 7.61 (4-H, 1H, d, *J* = 9.5 Hz), 7.35 (5-H, 1H, d, *J* = 8.6 Hz), 6.81 (6-H, 1H, d, *J* = 8.6 Hz), 5.42 (3′-H, 1H, d, *J* = 5.0 Hz), 6.61 (4′-H, 1H, d, *J* = 5.0 Hz), 1.45 (5′-H, 3H, s), 1.49 (6′-H, 3H, s), 6.14 (3″-H, 1H, q, *J* = 7.2 Hz), 1.97 (4″-H, 3H, d, *J* = 7.2 Hz), 1.88 (5″-H, 3H, s), 2.12 (2‴-H, 3H, s)
3	6.23 (3-H, 1H, d, *J* = 9.5 Hz), 7.60 (4-H, 1H, d, *J* = 9.5 Hz), 7.37 (5-H, 1H, d, *J* = 8.6 Hz), 6.82 (6-H, 1H, d, *J* = 8.6 Hz), 5.46 (3′-H, 1H, d, *J* = 5.0 Hz), 6.72 (4′-H, 1H, d, *J* = 5.0 Hz), 1.47 (5′-H, 3H, s), 1.51 (6′-H, 3H, s), 6.13 (3″-H, 1H, q, *J* = 7.2 Hz), 2.00 (4″-H, 3H, d, *J* = 7.2 Hz), 1.87 (5″-H, 3H, s), 6.03 (3‴-H, 1H, q, *J* = 7.2 Hz), 1.98 (4‴-H, 3H, d, *J* = 7.2 Hz), 1.85 (5‴-H, 3H, s)
4	6.25 (3-H, 1H, d, *J* = 9.6 Hz), 7.60 (4-H, 1H, d, *J* = 9.6 Hz), 7.35 (5-H, 1H, d, *J* = 8.6 Hz), 6.81 (6-H, 1H, d, *J* = 8.6 Hz), 5.41 (3′-H, 1H, d, *J* = 4.8 Hz), 6.63 (4′-H, 1H, d, *J* = 4.8 Hz), 1.45 (5′-H, 3H, s), 1.48 (6′-H, 3H, s), 6.13 (3″-H, 1H, q, *J* = 7.2 Hz), 1.98 (4″-H, 3H, d, *J* = 7.2 Hz), 1.89 (5″-H, 3H, s), 2.20, 2.28 (2‴-H, each 1H, m), 2.14 (3‴-H, 1H, m), 0.97 (4‴-H, 5‴-H, 6H, d, *J* = 7.2 Hz)
5	6.24 (3-H, 1H, d, *J* = 9.6 Hz), 7.60 (4-H, 1H, d, *J* = 9.6 Hz), 7.37 (5-H, 1H, d, *J* = 8.6 Hz), 6.82 (6-H, 1H, d, *J* = 8.6 Hz), 5.37 (3′-H, 1H, d, *J* = 4.8 Hz), 6.65 (4′-H, 1H, d, *J* = 4.8 Hz), 1.45 (5′-H, 3H, s), 1.48 (6′-H, 3H, s), 2.11 (2″-H, 3H, s), 6.03 (3‴-H, 1H, q, *J* = 7.2 Hz), 2.01 (4‴-H, 3H, d, *J* = 7.2 Hz), 1.88 (5‴-H, 3H, s)
6	6.25 (3-H, 1H, d, *J* = 9.6 Hz), 7.61 (4-H, 1H, d, *J* = 9.6 Hz), 7.36 (5-H, 1H, d, *J* = 8.6 Hz), 6.81 (6-H, 1H, d, *J* = 8.6 Hz), 5.34 (3′-H, 1H, d, *J* = 4.8 Hz), 6.57 (4′-H, 1H, d, *J* = 4.8 Hz), 1.42 (5′-H, 3H, s), 1.46 (6′-H, 3H, s), 2.26, 2.25 (2″-H, each 1H, m), 2.10 (3″-H, 1H, m), 0.98 (4″-H, 5″-H, each 3H, d, *J* = 7.2 Hz), 2.15 (2‴-H, 3H, s)
7	6.23 (3-H, 1H, d, *J* = 9.5 Hz), 7.59 (4-H, 1H, d, *J* = 9.5 Hz), 7.36 (5-H, 1H, d, *J* = 8.6 Hz), 6.81 (6-H, 1H, d, *J* = 8.6 Hz), 5.42 (3′-H, 1H, d, *J* = 4.8 Hz), 6.67 (4′-H, 1H, d, *J* = 4.8 Hz), 1.46 (5′-H, 3H, s), 1.50 (6′-H, 3H, s), 6.13 (3″-H, 1H, q, *J* = 7.2 Hz), 1.98 (4″-H, 3H, d, *J* = 7.2 Hz), 1.86 (5″-H, 3H, s), 5.63 (2‴-H, 1H, s), 1.89 (4‴-H, 3H, s), 2.20 (5‴-H, 3H, s)
8	6.24 (3-H, 1H, d, *J* = 9.6 Hz), 7.60 (4-H, 1H, d, *J* = 9.6 Hz), 7.36 (5-H, 1H, d, *J* = 8.6 Hz), 6.81 (6-H, 1H, d, *J* = 8.6 Hz), 5.34 (3′-H, 1H, d, *J* = 4.8 Hz), 6.57 (4′-H, 1H, d, *J* = 4.8 Hz), 1.45 (5′-H, 3H, s), 1.47 (6′-H, 3H, s), 2.30, 2.20 (2″-H, each 1H, m), 2.15 (3″-H, 1H, m), 0.98 (4″-H, 5″-H, 6H, d, *J* = 7.2 Hz), 2.30, 2.20 (2‴-H, each 1H, m), 2.15 (3‴-H, 1H, m), 0.98 (4‴-H, 5‴-H, 6H, d, *J* = 7.2 Hz)
9	6.27 (3-H, 1H, d, *J* = 9.5 Hz), 7.67 (4-H, 1H, d, *J* = 9.5 Hz), 7.35 (5-H, 1H, d, *J* = 8.6 Hz), 6.83 (6-H, 1H, d, *J* = 8.6 Hz), 5.28 (3′-H, 1H, d, *J* = 4.1 Hz), 5.09 (4′-H, 1H, d, *J* = 4.1 Hz),1.42 (5′-H, 3H, s), 1.45 (6′-H, 3H, s), 6.11 (3″-H, 1H, q, *J* = 7.2 Hz), 1.92 (4″-H, 3H, d, *J* = 7.2 Hz), 1.85 (5″-H, 3H, s)
10	6.33 (3-H, 1H, d, *J* = 9.6 Hz), 7.61 (4-H, 1H, d, *J* = 9.6 Hz), 7.56 (5-H, 1H, d, *J* = 8.6 Hz), 6.89 (6-H, 1H, d, *J* = 8.6 Hz), 5.68 (3′-H, 1H, s), 1.43 (5′-H, 3H, s), 1.60 (6′-H, 3H, s), 6.22 (3″-H, 1H, q, *J* = 7.2 Hz), 2.05 (4″-H, 3H, d, *J* = 7.2 Hz), 1.98 (5″-H, 3H, s)
11	6.23 (3-H, 1H, d, *J* = 9.5 Hz), 7.61 (4-H, 1H, d, *J* = 9.5 Hz), 7.35 (5-H, 1H, d, *J* = 8.6 Hz), 6.82 (6-H, 1H, d, *J* = 8.6 Hz), 5.30 (3′-H, 1H, d, *J* = 4.1 Hz), 6.16 (4′-H, 1H, d, *J* = 4.1 Hz), 1.41 (5′-H, 3H, s), 1.48 (6′-H, 3H, s), 6.12 (3‴-H, 1H, q, *J* = 7.2 Hz), 2.00 (4‴-H, 3H, d, *J* = 7.2 Hz), 1.86 (5‴-H, 3H, s)
12	6.25 (3-H, 1H, d, *J* = 9.5 Hz), 7.62 (4-H, 1H, d, *J* = 9.5 Hz), 7.38 (5-H, 1H, d, *J* = 8.6 Hz), 6.84 (6-H, 1H, d, *J* = 8.6 Hz), 5.30 (3′-H, 1H, d, *J* = 4.1 Hz), 6.18 (4′-H, 1H, d, *J* = 4.1 Hz),1.39 (5′-H, 3H, s), 1.46 (6′-H, 3H, s), 2.12 (2″-H, 3H, s), 1.23,1.20 (3‴, 4‴-H, each 3H, d, *J* = 6.6 Hz)
13	6.24 (3-H, 1H, d, *J* = 9.5 Hz), 7.61 (4-H, 1H, d, *J* = 9.5 Hz), 7.38 (5-H, 1H, d, *J* = 8.6 Hz), 6.29 (6-H, 1H, d, *J* = 8.6 Hz), 5.34 (3′-H, 1H, s), 1.40 (5′-H, 3H, s), 1.47 (6′-H, 3H, s), 2.12 (2″-H, 3H, s), 6.08 (3‴-H, 1H, q, *J* = 7.2 Hz), 2.02 (4‴-H, 3H, d, *J* = 7.2 Hz), 1.86 (5‴-H, 3H, s)
14	6.38 (3-H, 1H, d, *J* = 9.6 Hz), 7.77 (4-H, 1H, d, *J* = 9.5 Hz), 7.33 (5-H, 1H, s), 7.69 (2′-H, 1H, d, *J* = 2.2 Hz), 6.82 (3′-H, 1H, d, *J* = 2.2 Hz), 4.30 (-OCH_3, 3H, s)
15	6.29 (3-H, 1H, d, *J* = 9.6 Hz), 8.13 (4-H, 1H, d, *J* = 9.6 Hz), 7.63 (2′-H, 1H, d, *J* = 2.3 Hz), 7.00 (3′-H, 1H, d, *J* = 2.3 Hz), 4.17 (6H, s, 2× -OCH_3)
16	7.64 (3-H, 1H, d, *J* = 9.5 Hz), 6.26 (4-H, d, *J* = 9.5 Hz), 7.36 (5-H, 1H, d, *J* = 8.4 Hz), 6.78 (6-H, 1H, dd, *J* = 8.4, 2.2 Hz), 6.80 (8-H, 1H, d, *J* = 2.2 Hz)
17	5.35 (6-H, 1H, br s, *J* = 2.6 Hz), 5.15 (22-H, 1H, dd, *J* = 8.7, 15.2 Hz), 5.02 (23-H, 1H, dd, *J* = 8.7, 15.2 Hz), 3.56 (3-H, 1H, m), 2.31–1.04 (CH or CH_2), 1.00 (19-CH_3, 3H, s), 0.92 (26-CH_3, 3H, d, *J* = 6.9 Hz), 0.84 (28-CH_3, 3H, t, *J* = 7.5 Hz), 0.69 (22-CH_3, 3H, d, *J* = 6.4 Hz), 0.68 (29-CH_3, 3H, d, *J* = 7.6 Hz)
18	2.35, 1.63, 1.25 (t, CH_3)

and the biosynthesis raw material of its derivates. Moreover, the signals of *cis*-3′-acetyl-4′-angeloylkhellactone (**5**), *cis*-3′-isovaleryl-4′-acetylkhellactone (**6**), *cis*-3′-angeloyl-4′-senecioylkhellactone (**7**) and *cis*-3′,4′-diisovalerylkhellactone (**8**) were also observed at δ 6.65 (4′-H, d, *J* = 4.8 Hz), 6.56 (4′-H, d, *J* = 4.8 Hz), 6.67 (4′-H, d, *J* = 4.8 Hz) and 6.57 (4′-H, d, *J* = 4.8 Hz) in the spectrum, respectively (Fig. 2).

Some *trans*-type APs were also purified from this medicinal herb [33]. In comparison with *cis*-type ones, the coupling constant between H-3′ and H-4′ was around 4.1 Hz which was lower than those *cis*-khellactone derivates due to the *trans*-configuration between C-3′ and C-4′. By comparing the spectra of reference compounds, *trans*-3′-angeloylkhellactone (**9**), *trans*-4′-angeloylkhellactone (**10**), *trans*-3′-acetyl-4′-isobutyrylkhellactone (**11**) and *trans*-3′-acetyl-4′-angeloylkhellactone (**12**) were also identified according to the diagnostic signals at δ 7.67 (4-H, 1H, d, *J* = 9.5 Hz), 6.33 (3-H, d, *J* = 9.6 Hz), 6.16 (4′-H, d, *J* = 4.1 Hz) and 6.25 (3-H, d, *J* = 9.5 Hz), respectively, in the crude extract (Fig. 2). Besides the conspicuous signals, the rest signals were assigned in the assistance of various 2D NMR techniques.

The presence of 3′-angeloyloxy-4′-oxo-3′,4′-dihydroseselin (**13**) was confirmed by the distinct signal of H-3′ that was afforded as a doublet peak at δ 6.29 (6-H, 1H, d, *J* = 9.5 Hz) (Fig. 2), and the other signals of this compound were assigned using COSY, NOESY, TOCSY, HMQC, and HMBC spectra, and by comparing with the spectrum of reference compound.

In fact, some linear-type furanocoumarins were also extracted from Peucedani Radix [34], such as 5-methoxycoumarin (**14**) and 5,8-dimethoxycoumarin (**15**). The existence of 5,8-dimethoxycoumarin was confirmed on the basis of the double signals at δ 8.13 (4-H, d, *J* = 9.5 Hz) (Fig. 2). Moreover, the signal that were assigned to 5-methoxycoumarin were exhibited at δ 7.77 (4-H, d, *J* = 9.5 Hz) (Fig. 2). As the marker for the Umbelliferae plants, the characteristic signal of umbelliferone (7-hydroxylcoumarin, **16**) was also showed at δ 7.64 (3-H, d, *J* = 9.5 Hz) in the NMR spectrum of the extract (Fig. 2).

Fatty acids and steriols were widely distributed in plants. In the extract of Qian-hu, stigmasterol (**17**) and palmitic acid (**18**) were identified based on their protonic signals. Characteristic singlets of CH_3-18 in the sterols were observed at about δ 0.70, and the presence of stigmasterol (CH_3-18 at δ 0.68) was confirmed in comparison with the purified standards. In addition, fatty acid, such as palmitic acid was also detected and identified on the basis of the resonances at δ 2.35 (m, CH_2), 1.27 [m, $(CH_2)_n$], 1.62 (m, CH_2), and 0.90 (t, *J* = 6.6 Hz, CH_3) and the reference compound.

3.2. Multivariate statistical analysis

Following the assignments of the NMR spectra, chemical classification of Peucedani Radix was performed by multivariate data analysis, aiming to highlight the similarities or differences among these crude drugs from different districts. The ^{1}H NMR spectra of all extract samples were elucidated (Supplemental figures, Fig. S19), and the data files were introduced to Simca-P$^+$ software, respectively. An unsupervised approach by a principal component analysis (PCA), which is a multivariate projection method which extracts and displays systemic variation from a set of matrix data consisting of observations and variables [35] was applied to the ^{1}H NMR data set to group the plants according to the ^{1}H NMR signals characteristic (Fig. 3). Unit variance (UV) scaling methods were

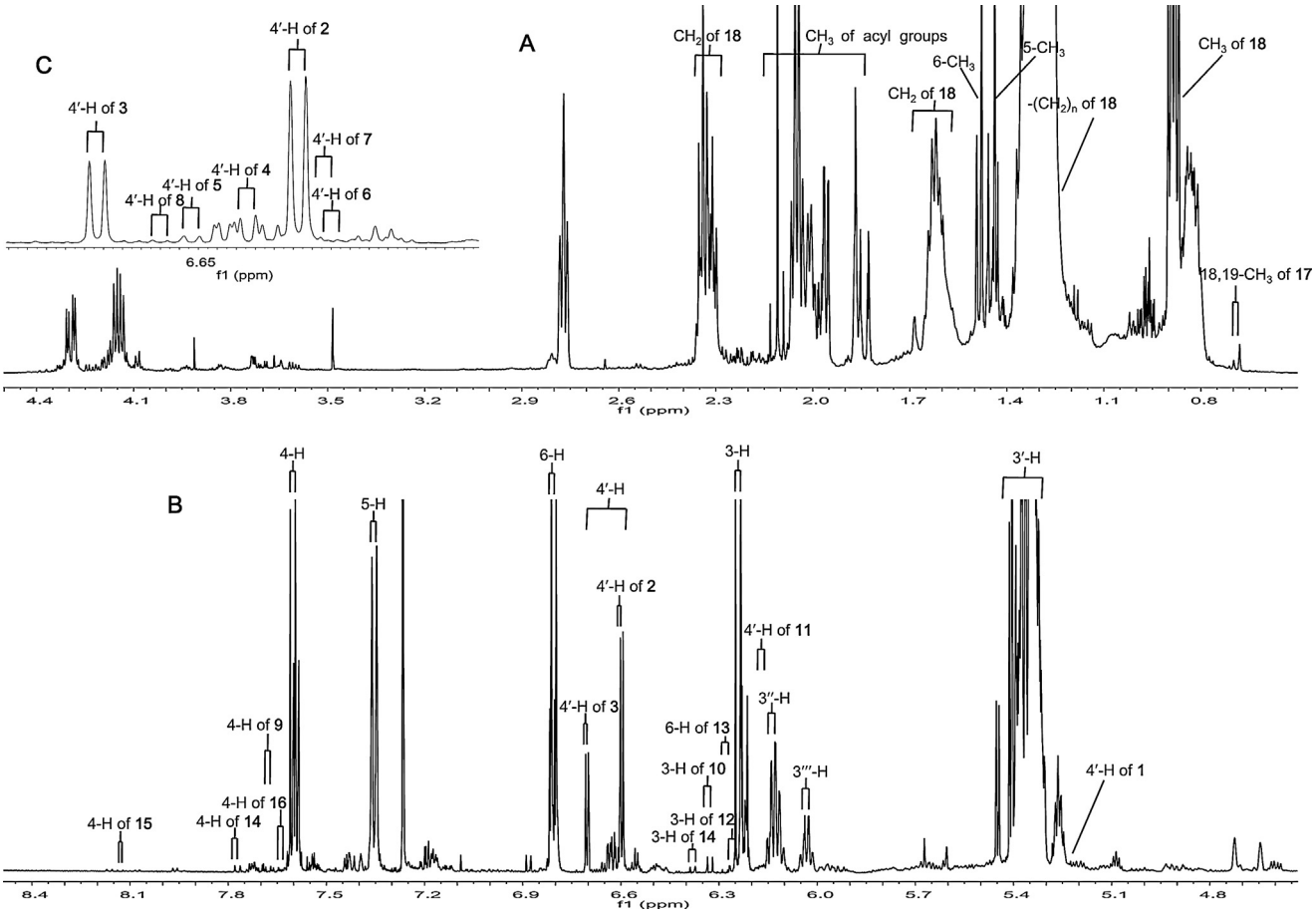

Fig. 2. Representative ^{1}H NMR spectra of Peucedani Radix, and the assignment of characteristic signals of compound **1**–**18** and angular-type pyranocoumarins. (A) The range of δ 0.5–4.5; (B) the range of δ 4.5–8.5; (C) the range of δ 6.50–6.75.

applied for PCA. A 19-component model explained 99.6% of the variance, with the first two components explaining 59.8%. The scatter plot clearly revealed that these crude materials from different locations could be divided into two groups I and II (Fig. 3A), indicating that the metabolic profiles of PR7, PR8 and PR15 (Group II) were quite different from the other batches which were grouped into in Group I (Supplemental figures, Fig. S19). Correspondingly, obvious difference could be observed for the ^{1}H NMR spectra between PR7-8 & 15 (Supplemental figures, Fig. S19) and the other samples. In the case of PR7, a group of unique signals was observed at δ 6.8–7.2, while these peaks could not be observed in the other samples. On the other side, all the signals between δ 6.0 and δ 8.0 (phenolic region) of PR-8 were quite lower than the other extracts, indicating that the contents of angular-type pyranocoumarins were the lowest in all the test samples. Moreover, the holistic metabolic profile of PR15, in particular the regions of δ 5.7–7.0 and δ 3.5–4.0, was significantly distinct from PR1–14. Thus, it is not surprising that PR15 located at the third quadrant solely.

The loadings plot (Fig. 3B) of PC1 and PC2 was used to find the metabolites that are responsible for the separation between these two groups. The signals of the angular-type pyranocoumarins at δ 1.45, 1.49, 1.85, 1.89, 1.93, 2.01, 2.05, 2.09, 5.30, 5.42, 6.06, 6.22, 6.26, 6.82, 7.34, 7.38 and 7.58 were observed as the main markers to distinct groups I and II (Fig. 3B). Furthermore, the signals that belong to fatty acids and steriols were also regarded as the markers due to the signals of δ 0.81, 0.85, 0.89, 1.13, 1.41, 1.58, 1.61, 2.29, 2.33 and 5.26, and the signal of δ 6.34 was assigned to compound **14**, which is widely distributed in Apiaceae (Umbelliferae) herbs. In addition, the signal of δ 2.77 also played an important role for the distinction of groups I and II, but the signal could not be unambiguously assigned with the assistance of reference compounds and various 2D spectra. Above all, in view of the extensive activities of APs related to the effect of Qian-hu, this type of coumarins along with 5-methoxycoumarin was regarded as the markers that were responsible for the distinction of 15 batches of Peucedani Radix. As we mentioned above, PA and PB were the major constituents in all APs, thus it is reasonable to believe that these two components played principal roles.

3.3. Quantitative analysis

As chloroform was documented as the solvent for the extraction of Peucedani Radix [1], so, in current study, $CHCl_3$ was adopted as the extraction solvent. Reflux and ultrasonic bath extraction are two universally used extraction methods for many Chinese medicines. Since there is no obvious difference for the extraction efficacy of PA and PB by these two means, ultrasonic bath extraction was finally selected due to its convenient operation process. Additionally, the extraction duration were optimized for obtaining the highest extraction efficacy and the results revealed no difference between the extraction efficacy of 30 min and 60 min. Furthermore, extraction cycles have been optimized as one cycle. Therefore, the pulverized herbal materials were extracted with chloroform in ultrasonic bath method for 30 min by once cycle.

APs owned a quite similar skeleton and the ^{1}H NMR peaks of these constituents might interfere with each other. In order to analyze these PAs efficiently and simultaneously, couples of solvent systems were served as the candidates for the detection. And then,

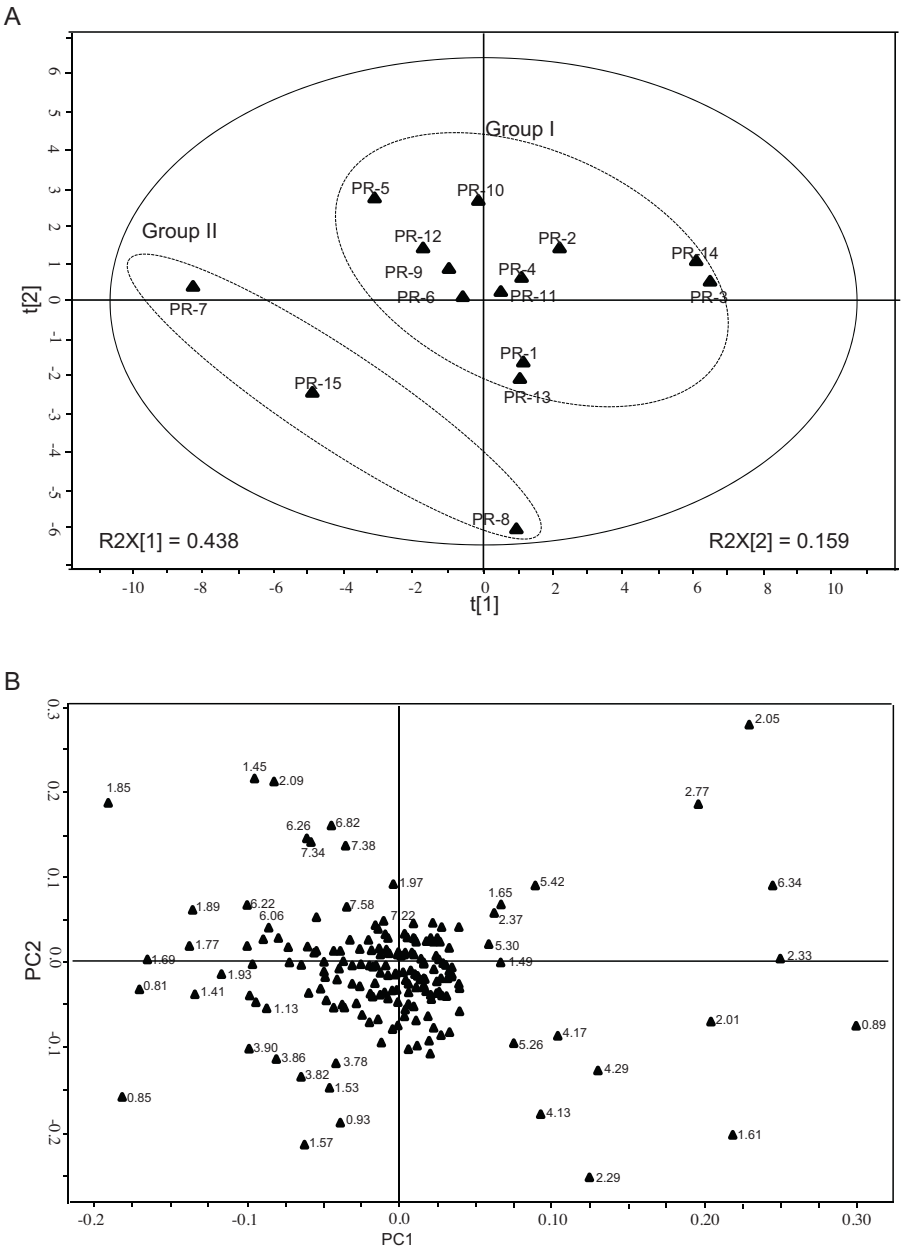

Fig. 3. Principle component analysis (PCA) results of ^{1}H NMR spectra of Peucedani Radix (PR1–15) based on the whole range of δ 0.5–8.5. (A) The score plot of PCA; (B) the loading scatter plot of PCA.

the results revealed that $CDCl_3$ could be chosen as optimal solvent to offer well dissolubility and give well separation of target peaks originating from these pyranocoumarins.

In the ^{1}H NMR-based quantification of praeruptorin A and praeruptorin B in Peucedani Radix, it would be desirable to quantify each individual coumarin by means of the integral value of a specific proton signal. The H-4′ signals of these APs resonating in a specific region of spectra as a doublet peak with little interference were specific for these coumarins and thus could be accepted as the target signal for the quantitation of PA and PB in the present study. The doublet signal at δ 6.61 (4′-H) with a coupling constant as 5.0 Hz was selected to determine the concentration of praeruptorin A (Fig. 4), while the characteristic double signal at δ 6.72 (4′-H) with a coupling constant as 5.0 Hz in the protonic NMR spectra were employed as the quantitative peak for praeruptorin B (Fig. 4).

In the process of q^{1}H NMR analysis, a suitable internal standard is always necessary. The appropriate internal standard should be preferably a stable compound with a sharp signal in a non crowded region of the ^{1}H NMR spectrum. Based on these requirements, formononetin, with a characteristic singlet signal at δ 7.90 (2-H) in the ^{1}H NMR spectroscopy (Fig. 4) and a constant integral value within 48 h, was adopted as the internal standard in this assay.

In the case of ^{1}H NMR quantitative analysis, calibration curves are not needed for quantification of the compounds because integration of the peaks is always proportional to the amount of the compound and is always the same for all compounds. However, calibration curves for each analyte were determined in the range of 0.039–5.00 mg/mL in order to check the linearity of the method. The calibration curve of PA was $y = 6.594x - 0.164$ ($R^2 = 0.997$), where x represented concentration while y meant the integral area of signal at H-4′, while that of PB was $y = 5.595x - 0.065$ ($R^2 = 0.997$).

The recovery tests were analyzed by the method described above, and the results revealed that the recoveries of praeruptorin A and praeruptorin B were in the range of 92.10–107.30%. The LOD

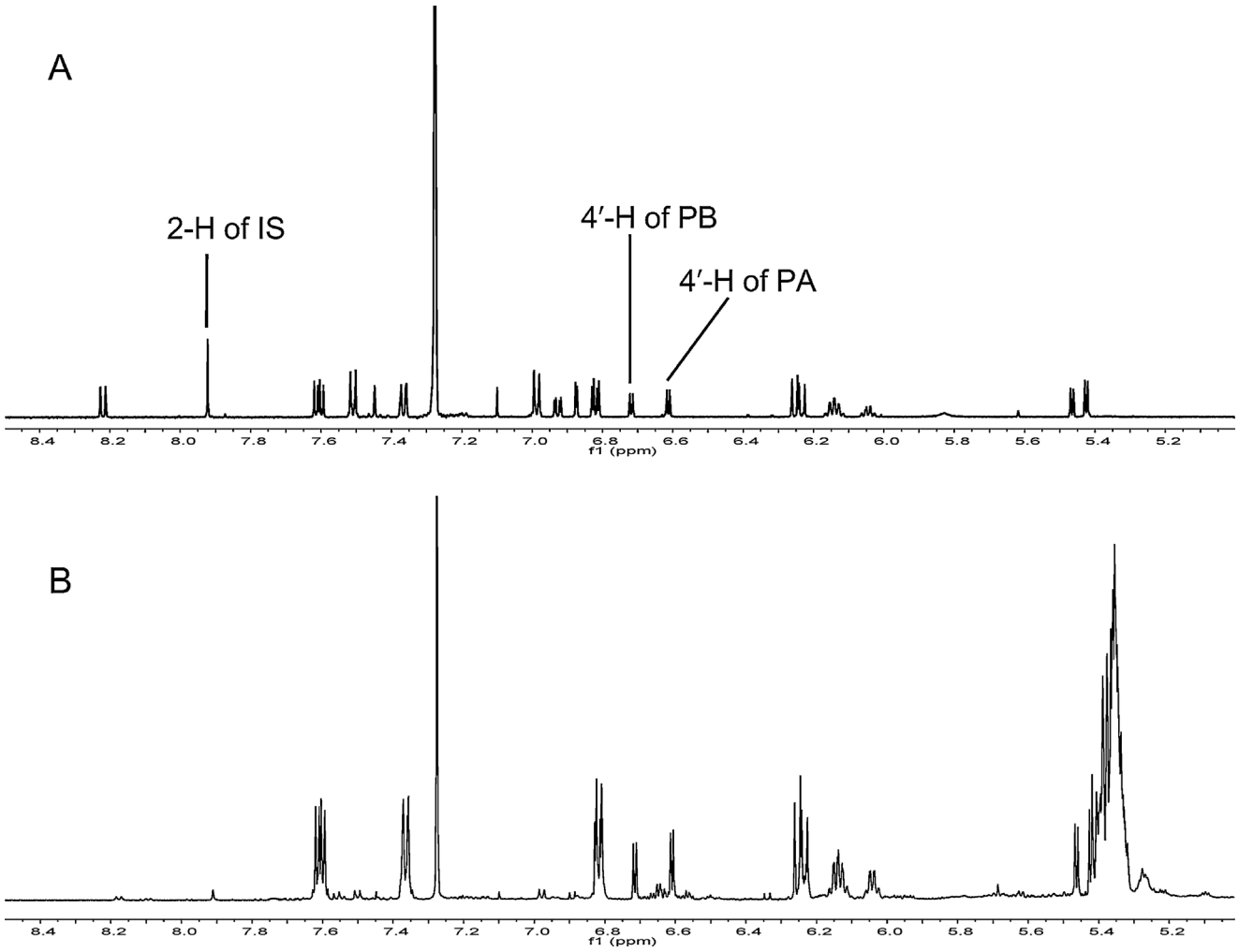

Fig. 4. Representatively quantitative ^{1}H NMR spectra. (A) Mixed standards (PA + PB, each 156 μg/mL) plus with 150 μg/mL internal standard (IS); (B) PR1 plus with 150 μg/mL internal standard (IS).

for PA and PB was 39.1 μg/mL and the LOQ was 19.5 μg/mL, respectively. The RSDs of precision and repeatability tests are both below 3%. The stability results proved that the sample could keep stable within 24 h. All the data above demonstrated that this proposed method is highly accurate and precise.

The contents of PA and PB in each studied plant sample were showed in Table 1. The concentrations of these two analytes in the Peucedani Radix evaluated using the presented method showed big variations among 15 batches of Qian-hu. PA was not detected in PR12 and PR15, while PB was absent in PR7, PR12 and PR15. The contents of praeruptorin A in PR1–5, 10–11 and 13–14 were more than 0.9%, which was the standard documented in Chinese Pharmacopoeia [1]. For the other chemical indicator of Qian-hu, the contents of PB in PR6, PR8 and PR9 were lower than the 0.24%, indicating that these batches could not meet the requirement of authoritative standard.

As we described in Section 3.3, PR7, PR8 and PR15 were grouped away from the other samples, but the determination results suggested PR9 and PR12 were also quite different from the other samples in Group I. The metabolocomic study of Qian-hu concerned about the overall metabolic profile of crude extract, while the q^{1}H NMR assay was just focused on the contents of PA and PB. Therefore, more chemical indicators were suggested to be included for the quality control of this herbal medicine.

4. Conclusions

This NMR method is simple and rapid, specific, no reference compounds are needed, apart from the cheap internal standard, and an overall profile of the preparation can be obtained directly. With the assistance of NMR spectroscopy and multivariate statistical analysis, metabolomic characterization was achieved and angular-type pyranocoumarins along with 5-methoxycoumarin were revealed as the main chemical markers being responsible to distinct Peucedani Radix from different districts. Meanwhile, the contents of PA and PB could also be simultaneously determined using q^{1}H NMR spectroscopy within much shorter time than by the conventional chromatographic or other analysis methods reported. Therefore, the developed ^{1}H NMR method can be used as a rapid and convenient means for the quality control of Qian-hu, including identification of Peucedani Radix based on overall profile and simultaneous quantification of praeruptorin A and praeruptorin B using q^{1}H NMR.

Supplementary information

The supplemental ^{1}H NMR spectra of compounds **1**–**18** and all the ^{1}H NMR spectra of 15 batches of Peucedani Radix (PR1–15) are available in supplementary data.

Acknowledgement

The research was supported by the National Basic Research Program of China 973 program (Grant No. 2009CB522707).

Appendix A. Supplementary data

Supplementary data associated with this article can be found, in the online version, at http://dx.doi.org/10.1016/j.jpba.2013.08.021.

References

[1] The State Pharmacopoeia Commission of P.R. China, *Radix Peucedani* Pharmacopoeia of the People's Republic of China, Vol. I, Chemical Industry Press, Beijing, China, 2010, pp. 248.
[2] H.M. Chang, P.P.H. But, S.C. Yao, L.L. Wang, S.C.S. Yeung, Pharmacology and Applications of Chinese Materia Medica, Vol. 2, World Scientific Publisher, Singapore, 2001, pp. 905.
[3] N.C. Zhao, W.B. Jin, X.H. Zhang, F.L. Guan, Y.B. Sun, H. Adachi, T. Okuyama, Relaxant effects of pyranocoumarin compounds isolated from a Chinese medical plant, Bai-Hua Qian-Hu, on isolated rabbit tracheas and pulmonary arteries, Biol. Pharm. Bull. 22 (1999) 984–987.
[4] T.H. Chang, H. Adachi, T. Okuyama, K.Y. Zhang, Effects of 3′-angeloyloxy-4′-acetoxy-3′,4′-dihydroseselin on myocardial dysfunction after a brief ischemia in anesthetized dogs, Acta Pharmcol. Sin. 15 (1994) 388–391.
[5] T. Okuyama, M. Takata, H. Nishino, A. Nishino, J. Takayasu, A. Iwashima, Studies on the antitumor-promoting activity of naturally occurring substances. II. Inhibition of tumor-promoter-enhanced phospholipid metabolism by umbelliferous materials, Chem. Pharm. Bull. (Tokyo) 38 (1990) 1084–1086.
[6] Y.Y. Xiong, F.H. Wu, J.S. Wang, J. Li, L.Y. Kong, Attenuation of airway hyperreactivity and T helper cell type 2 responses by coumarins from *Peucedanum praeruptorum* Dunn in a murine model of allergic airway inflammation, J. Ethnopharmacol. 141 (2012) 314–321.
[7] L.Y. Kong, Y.H. Pei, X. Li, T.R. Zhu, Studying progress on the coumarins of khellactone derivatives, Tianran Chanwu Yanjiu Yu Kaifa 6 (1994) 51–65.
[8] S.L. Zhang, J.M. Li, Q.H. Xiao, A.H. Wu, Q. Zhao, G.R. Yang, K.Y. Zhang, Effect of dl-praeruptorin A on ATP sensitive potassium channels in human cortical neurons, Acta. Pharmacol. Sin. 22 (2001) 813–816.
[9] T. Liang, W. Yue, Q. Li, Chemopreventive effects of *Peucedanum praeruptorum* DUNN and its major constituents on SGC7901 gastric cancer cells, Molecules 15 (2010) 8060–8071.
[10] W.F. Fong, J.X. Zhang, J.Y. Wu, K.W. Tse, C. Wang, H.Y. Cheung, M.S. Yang, Pyranocoumarin (±)-4′-O-acetyl-3′-O-angeloyl-cis-khellactone induces mitochondrial-dependent apoptosis in HL-60 cells, Planta Med. 70 (2004) 489–495.
[11] X. Shen, G. Chen, G. Zhu, W.F. Fong, (±)-3′-O,4′-O-Dicynnamoyl-cis-khellactone, a derivative of (±)-praeruptorin A, reverses P-glycoprotein mediated multidrug resistance in cancer cells, Bioorg. Med. Chem. 14 (2006) 7138–7145.
[12] J.Y. Wu, W.F. Fong, J.X. Zhang, C.H. Leung, H.L. Kwong, M.S. Yang, D. Li, H.Y. Cheung, Reversal of multidrug resistance in cancer cells by pyranocoumarins isolated from *Radix Peucedani*, Eur. J. Pharmacol. 473 (2003) 9–17.
[13] Y. Aida, T. Kasama, N. Takeuchi, S. Tobinaga, The antagonistic effects of khellactones on platelet-activating factor, histamine, andleukotriene D4, Chem. Pharm. Bull. 43 (1995) 859–867.
[14] Y.Y. Xiong, J.S. Wang, F.H. Wu, J. Li, L.Y. Kong, The effects of (±)-Praeruptorin A on airway inflammation, remodeling and transforming growth factor-β1/Smad signaling pathway in a murine model of allergic asthma, Int. Immunopharmacol. 14 (2012) 392–400.
[15] Y. Xiong, J. Wang, F. Wu, J. Li, L. Zhou, L. Kong, Effects of (±)-praeruptorin A on airway inflammation, airway hyperresponsiveness and NF-κB signaling pathway in a mouse model of allergic airway disease, Eur. J. Pharmacol. 683 (2012) 316–324.
[16] L. Yang, X.B. Li, Q. Yang, K. Zhang, N. Zhang, Y.Y. Guo, B. Feng, M.G. Zhao, Y.M. Wu, The neuroprotective effect of praeruptorin C against NMDA-induced apoptosis through down-regulating of GluN2B-containing NMDA receptors, Toxicol. In Vitro 27 (2013) 908–914.
[17] H. Nishino, T. Okuyama, M. Takata, S. Shibata, H. Tokuda, J. Takayasu, T. Hasegawa, A. Nishino, H. Ueyama, A. Iwashima, Studies on the anti-tumor-promoting activity of naturally occurring substances. IV. Pd-II [(+)anomalin, (+)praeruptorin B], a seselin-type coumarin, inhibits the promotion of skin tumor formation by 12-O-tetradecanoylphorbol-13-acetate in 7,12-dimethylbenz[a]anthracene-initiated mice, Carcinogenesis 11 (1990) 1557–1561.
[18] P.J. Yu, H. Jin, J.Y. Zhang, G.F. Wang, J.R. Li, Z.G. Zhu, Y.X. Tian, S.Y. Wu, W. Xu, J.J. Zhang, S.G. Wu, Pyranocoumarins isolated from *Peucedanum praeruptorum* Dunn suppress lipopolysaccharide-induced inflammatory response in murine macrophages through inhibition of NF-κB and STAT3 activation, Inflammation 35 (2012) 967–977.
[19] D. Bertelli, G. Papotti, L. Bortolotti, G.L. Marcazzan, M. Plessia, ^{1}H NMR simultaneous identification of health-relevant compounds in propolisextracts, Phytochem. Anal. 23 (2012) 260–266.
[20] E.M. Lenz, I.D. Wilson, Analytical strategies in metabonomics, J. Proteome Res. 6 (2007) 443–458.
[21] M.Y. Wu, J.S. Ye, Q.X. Liu, Identification and studies on chemotaxonomy of Chinese crude drug "Qian-hu" by NMR spectroscopy, J. Plant Resour. Environ. 5 (1996) 14–17.
[22] Q.X. Liu, M.Y. Wu, G.X. Rao, J.S. Ye, H. Hui, Cemotaxonomy of Ferulineae based on the coumarins identified by ^{1}H NMR, J. Plant Resour. Environ. 8 (1999) 46–51.
[23] N.H. Wang, K. Baba, M. Taniguchi, Simple and convenient application of ^{1}H NMR method in the chemotaxonomy of Apioideae, J. Plant Resour. Environ. 5 (1996) 40–44.
[24] J.S. Ye, M.Y. Wu, Q.X. Liu, Identification and chemotaxonomy of 3 Chinese crude drug "Qian-hu" by NMR spectroscopy, J. Plant Resour. Environ. 4 (1995) 60–62.
[25] N.Q. Liu, Y.H. Choi, R. Verpoorte, F. van der Kooy, Comparative quantitative analysis of artemisinin by chromatography and qNMR, Phytochem. Anal. 21 (2010) 451–456.
[26] J. Staneva, P. Denkova, M. Todorova, L. Evstatieva, Quantitative analysis of sesquiterpene lactones in extract of *Arnica montana* L. by ^{1}H NMR spectroscopy, J. Pharm. Biomed. Anal. 54 (2011) 94–99.
[27] H.K. Kim, Y.H. Choi, W.T. Chang, R. Verpoorte, Quantitative analysis of ephedrine analogues from ephedra species using ^{1}H NMR, Chem. Pharm. Bull. 51 (2003) 1382–1385.
[28] E.C. Tatsis, V. Exarchou, A.N. Troganis, I.P. Gerothanassis, ^{1}H NMR determination of hypericin and pseudohypericin in complex natural mixtures by the use of strongly deshielded OH groups, Anal. Chim. Acta 607 (2008) 219–226.
[29] Y.L. Song, Q.W. Zhang, Y.P. Li, R. Yan, Y.T. Wang, Enantioseparation and absolute configuration determination of angular-type pyranocoumarins from Peucedani Radix using enzymatic hydrolysis and chiral HPLC–MS/MS analysis, Molecules 17 (2012) 4236–4251.
[30] F. Malz, H. Jancke, Validation of quantitative NMR, J. Pharm. Biomed. Anal. 38 (2005) 813–823.
[31] Z.X. Chen, B.S. Huang, Q.L. She, G.F. Zeng, The chemical constituents of Bai-hua-qian-hu, the root of *Peucedanum praeruptorum* Dunn. (umbelliferae) – four new coumarins, Yao Xue Xue Bao 14 (1979) 486–496.
[32] J.S. Ye, H.Q. Zhang, C.Q. Yuan, Isolation and identification of coumarin praeruptorin E from the root of the Chinese drug *Peucedanum praeruptorum* DUNN (umbelliferae), Yao Xue Xue Bao. 17 (1982) 431–434.
[33] M. Takata, S. Shibata, T. Okuyama, Structure of angular pyranocoumarins of Bai-Hua Qian-Hu, the root of *Peucedanum praeruptorum*, Planta Med. 56 (1990) 307–311.
[34] L.Y. Kong, Y.H. Pei, X. Li, T.R. Zhu, T. Okuyama, Isolation and structure elucidation of qianhucoumarin A, Yao Xue Xue Bao 28 (1993) 432–436.
[35] L. Eriksson, E. Johansson, N. Kettaneh-Wold, J. Tyrgg, C. Wikström, S. Wold, Multi- and Megavariate Data Analysis, Part 1: Basic Principles and Applications, second ed., Umetrics, Umeå, Sweden, 2006.